

引用格式: LU Ye, GONG Huaping, CAI Jingyi, et al. In-situ Calibration Method of FBG Strain Sensor under Dynamic Excitation[J]. Acta Photonica Sinica, 2023, 52(1):0106005

陆叶, 龚华平, 蔡静怡, 等. 动态激励下的 FBG 应变传感器原位校准方法[J]. 光子学报, 2023, 52(1):0106005

动态激励下的 FBG 应变传感器原位校准方法

陆叶¹, 龚华平¹, 蔡静怡¹, 樊其明², 赵春柳¹

(1 中国计量大学 光学与电子科技学院, 杭州 310018)

(2 中国计量科学研究院光学与激光计量科学研究所, 北京 100029)

摘 要:针对光纤光栅应变传感器测量桥梁结构动态应变值的准确性问题,提出了一种动态激励下的光纤光栅应变传感器的校准方法。采用等强度悬臂梁模拟桥梁结构,在等强度悬臂梁末端瞬间悬挂不同重量的砝码来模拟桥梁上汽车产生的动态激励。以电阻应变片作为参考传感器,光纤光栅应变传感器作为待校准传感器,将这两个传感器的测量数据序列进行比对。针对传感器的测量数据序列出现的时间错位问题,采用互相关算法对参考传感器和待校准传感器的测量数据进行数据匹配。在光纤光栅应变传感器有初始值的情况下进行测量值校准的研究。实验结果表明,该方法有效解决了测量数据序列的时间错位问题,实现了光纤光栅应变传感器的动态校准,采用不同重量的砝码作为激励源对校准结果没有影响,1529 nm 和 1547 nm 波长的光纤光栅应变传感器灵敏度校准系数与静态标定结果基本一致。

关键词: 光纤布拉格光栅; 动态校准; 数据序列匹配; 应变传感器; 数据错位

中图分类号: TB92

文献标识码: A

doi: 10.3788/gzxb20235201.0106005

0 引言

桥梁的健康状况对经济发展、交通运输和社会生活有显著影响,对桥梁进行健康监测至关重要,尤其是桥梁结构内部的应变监测。高性能、大规模分布式智能传感元件如光纤光栅传感元件为桥梁结构健康监测系统的发展提供了基础^[1-2]。光纤光栅(Fiber Bragg Grating, FBG)应变传感器具有抗电磁干扰能力强、精度高、耐久性好、可以分布式测量^[3-6]等优点。FBG 应变传感器在桥梁健康监测时,通常要在动态工况下工作,若传感器测量数据有误,将对后续的控制、监测以及故障诊断等系统产生不良影响,出现误诊断、误报警等现象,造成重大损失,因此要对实际使用中的 FBG 应变传感器进行现场校准,保证测量结果的准确性。

目前对于 FBG 应变传感器的现场校准主要有静态校准和动态校准两种方法^[7-12],在实际桥梁检测时,进行静态校准必须阻断交通运行一段时间,会对社会经济生活产生一定的影响,而动态校准对于交通运行几乎没有影响。金冉等^[10]提出了一种激光绝对法冲击校准装置,该校准装置采用霍普金森杆产生动态激励,实现了对应变传感器动态特性的校准,但装置较难实现固定或连续频率的加载方式,且爆炸冲击产生的高温也会对其标定结果产生一定的影响。YU S J 等^[11]设计了一种用于混凝土动态应变测量的光纤光栅传感器,通过动态应变储存系统输出 FBG 应变传感器和电阻应变片(Electronic Strain Gauge, ESG)传感器的测量结果并进行对比,完成动态标定。落锤法在瞬间可以产生巨大的荷载,但是很难在实验过程中产生恒定的荷载与应变,因此对 FBG 应变传感器的动态标定有一定的局限性。江承成等^[12]设计了一种振动台与等强度梁结合的 FBG 应变传感器的动态标定方案,将激光测振仪、加速度传感器、FBG 应变传感器三者的信号进行分析,实现了对传感器固定频率下长时间振动状态标定和一定频率段的扫频标定。

基金项目: 国家重点研发计划(No.2020YFF0217803)

第一作者: 陆叶, 1424680661@qq.com

通讯作者: 龚华平, gonghp@163.com

收稿日期: 2022-06-16; 录用日期: 2022-07-06

<http://www.photon.ac.cn>

本文采用等强度悬臂梁模拟桥梁结构,在等强度悬臂梁末端瞬间悬挂不同重量的砝码产生的动态激励来模拟桥梁上随机通行的汽车产生的动态应变,以电阻应变片作为参考传感器,FBG应变传感器作为待校准传感器,将这两个传感器的测量值进行比对。采用互相关算法对标准传感器和待校准传感器的测量数据进行数据匹配,解决传感器应变数据时间错位的问题,然后在有初始值情况下计算两者波峰的比值作为灵敏度校准系数。

1 实验装置

本文利用砝码作为激励源来模拟桥梁上随机通行的汽车载荷,建立参考传感器与待校准传感器对结构动态应变进行同步测量比对的校准模型。该校准模型由激励源、被测量结构物、参考传感器和待校准传感器组成。选择高精度电阻应变片作为参考传感器,电阻应变片的结构简单、输出精度高、稳定性较好,适合作为应变值传递的标准传感器使用。通过电阻应变测量仪测出电阻应变片的电阻变化值,便可得到待测结构物的准确应变值^[13]。

实验中,以电阻应变片作为参考传感器,FBG应变传感器作为待校准传感器,等强度悬臂梁模拟桥梁结构,悬挂砝码产生的瞬时应变提供动态激励。为确保FBG应变传感器和电阻应变片所测参量的一致,将FBG应变传感器与电阻应变片粘贴在等强度悬臂梁同一位置处,分别采用重量为250 g和500 g的砝码,瞬时悬挂在等强度悬臂梁末端,校准实验装置如图1所示。图1中,电阻应变片与FBG应变传感器并排近距离安装。数据采集单元为动态应变仪(XL2101B4)和动态FBG解调仪(SM130),分别用于实时获取电阻应变片的应变值和FBG应变传感器的输出波长值。FBG应变传感器为裸光纤光栅,3 dB带宽为0.2 nm,对比度为17 dB。动态应变仪的分辨率为0.1 $\mu\epsilon$,精度为1% $\pm 1 \mu\epsilon$,动态FBG解调仪的分辨率为0.1 pm,精度为 ± 2 pm,采样频率都设为100 Hz。

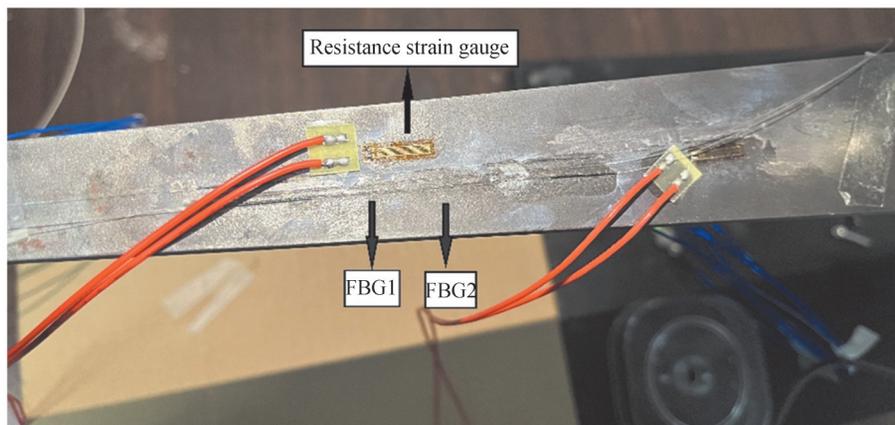


图1 FBG应变传感器动态校准实验装置

Fig.1 Diagram of FBG strain sensor dynamic calibration experimental device

将FBG应变传感器通过光纤光栅解调仪与上位机连接,电阻应变片通过电阻应变仪与上位机连接,动态校准系统框图如图2所示。在等强度悬臂梁末端悬挂砝码,砝码悬挂的瞬间产生动态激励作用于等强度悬臂梁,载荷传递至光纤FBG的光栅区域,导致FBG中心波长的变化,中心波长的变化值通过光纤光栅解调仪对反射光信号进行解调而得到,计算机上显示和记录FBG应变传感器的波长值,同时电阻应变片的实际应变值由电阻应变仪采集并传输到计算机上显示和记录。

首先在未悬挂砝码的情况下,先后打开数据采集软件采集电阻应变片和FBG应变传感器的初始值,其中FBG应变传感器采集时间约1 s,电阻应变片采集时间约3 s。然后在悬臂梁末端瞬间悬挂一个砝码,两个传感器同时采集约10 s,完成一次数据采集过程。分别采用250 g和500 g的砝码模拟不同的动态激励,重复三次上述实验过程,获得相应的数据文件。在实验室条件下,保持环境温度22℃不变,同时实验室基本没有环境振动噪声的影响。

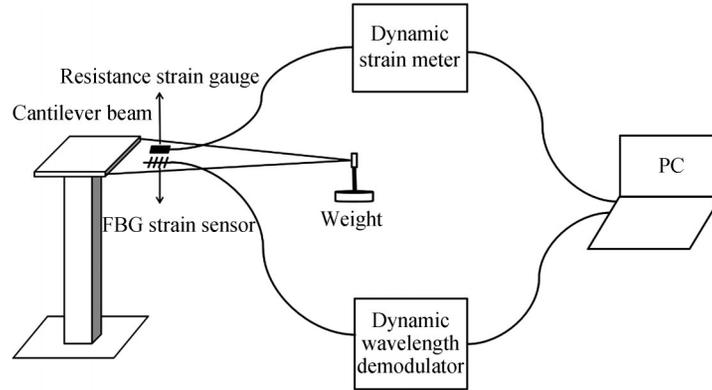


图2 FBG应变传感器动态校准系统
Fig.2 FBG strain sensor dynamic calibration system

2 波形匹配

由于参考传感器和待校准传感器采样开始时间不同步,两测量值序列的变化波形会出现时间错位。动态校准的前提是待校准传感器与参考传感器在相同激励源条件下的量值波形变化基本一致,如果两量值序列的波形匹配性较差,将无法进行传感器的动态校准。本实验采用互相关算法进行应变波形的数据序列匹配。在信号处理领域,互相关函数用于描述两个信号在两个不同时刻的取值的相关程度^[14-15],对于数据的匹配分析和数据波形的一致性判断具有良好的效果。通过互相关函数求出两组数据在相关性最大时的偏移量,然后移动其中一组数据序列从而将两组数据序列进行对齐。

实验分别采用波长为1 529 nm和1 547 nm的FBG应变传感器,重量为250 g和500 g的砝码瞬时悬挂等强度悬臂梁末端,以悬挂砝码三次的数据为例来说明动态校准方法的实验结果。实验过程中,保持温度为22℃,避免温度变化引起FBG应变传感器的波长漂移。图3为1 529 nm的FBG应变传感器与电阻应变片的波形匹配结果图。由图3可知,1 529 nm的FBG应变传感器与电阻应变片通过互相关算法可以较为准确地进行波形匹配。

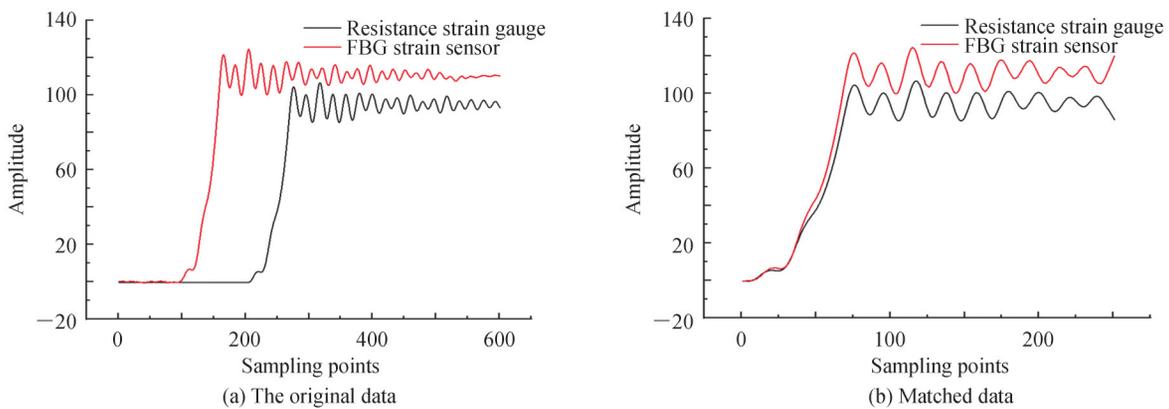


图3 1529 nm波长的FBG应变传感器与电阻应变片波形匹配结果
Fig.3 Waveform matching results of 1529 nm FBG strain sensor and resistance strain gauge

分别采用250 g和500 g砝码进行动态校准实验三次,三次实验的波形匹配系数计算结果如表1所示。

表1 1 529 nm和1 547 nm波长的FBG应变传感器波形匹配系数
Table 1 Waveform matching coefficient of FBG strain sensor at 1 529 nm and 1 547 nm

Weight/g	First test		Second test		Third test	
	1 529 nm	1 547 nm	1 529 nm	1 547 nm	1 529 nm	1 547 nm
250	0.994 9	0.994 8	0.989 5	0.989 4	0.991 3	0.991 1
500	0.996 4	0.996 4	0.983 8	0.983 5	0.996 4	0.996 3

可以看出波形匹配系数均大于0.98,大部分系数都达到0.99,表明FBG应变传感器与电阻应变片的测量数据具有高度一致性,这为下一步的传感器校准奠定了基础。

3 动态校准方法与结果

在未悬挂砝码的状态下,采集FBG应变传感器的初始波长值 λ_0 与电阻应变片的初始应变值 ϵ_0 。然后悬挂一个砝码进行动态数据采集,将FBG应变传感器的波长值 λ 与电阻应变片应变值 ϵ 分别转换为波长变化量 $\Delta\lambda$ 和应变变化量 $\Delta\epsilon$,即

$$\begin{cases} \Delta\lambda = \lambda - \lambda_0 \\ \Delta\epsilon = \epsilon - \epsilon_0 \end{cases} \quad (1)$$

FBG传感公式为

$$\Delta\lambda = k \cdot \Delta\epsilon + k_T \cdot \Delta T \quad (2)$$

式中, k 为FBG的应变灵敏度系数; k_T 为FBG的温度灵敏度系数。温度变化是影响FBG测量的重要因素,在温度不变的情况下进行研究,则FBG应变传感器受到的应变与波长呈线性关系,式(2)可简化为

$$\Delta\lambda = k \cdot \Delta\epsilon \quad (3)$$

假设FBG应变传感器波形曲线上的第一个波峰值为 λ_1 ,电阻应变片波形曲线上的第一个波峰值为 ϵ_1 ,计算其比值作为灵敏度校准系数,则灵敏度校准系数 k 为

$$k = \frac{\lambda_1 - \lambda_0}{\epsilon_1 - \epsilon_0} \quad (4)$$

用同样的方法对其余6个波峰值进行处理,共得到7个灵敏度校准系数,取平均值作为最终的灵敏度校准系数。图4为经过式(1)处理后的电阻应变片和FBG应变传感器的波形,将电阻应变片的波峰值和FBG应变传感器的波峰值代入式(4)进行灵敏度校准系数的计算。

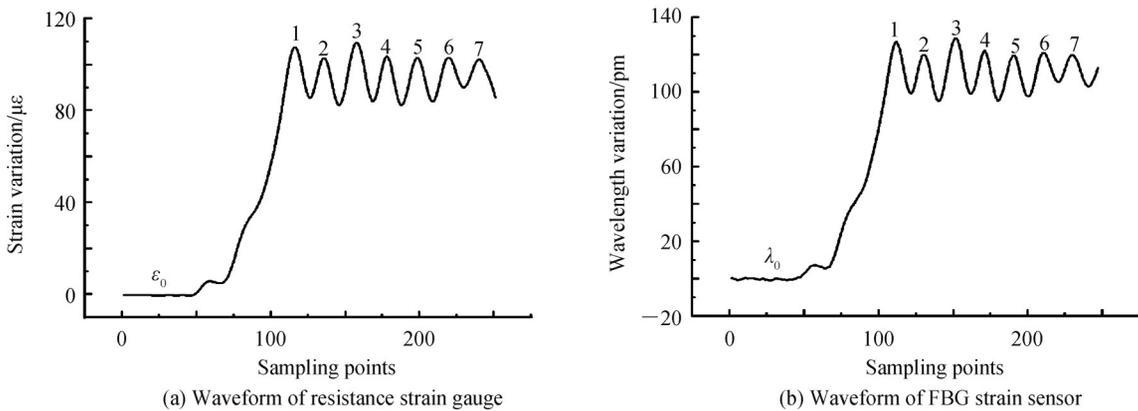


图4 电阻应变片与FBG应变传感器的波形

Fig.4 Waveform of resistance strain gauge and FBG strain sensor

在悬臂梁末端瞬间悬挂一个重量为250 g的砝码,1 529 nm和1 547 nm波长的FBG应变传感器和电阻应变片的波峰值分别如表2、表3所示,选取这7个波峰值计算其比值得到7个灵敏度系数,最后取这7个灵敏度系数的平均值作为1 529 nm和1 547 nm波长的FBG应变传感器的灵敏度校准系数,分别是1.23 pm/ $\mu\epsilon$ 和1.19 pm/ $\mu\epsilon$,其相对标准差仅为0.57%和0.88%。

表2 1 529 nm波长的FBG应变传感器和电阻应变片波峰值
Table 2 Peak value of FBG strain sensor and resistance strain gauge at 1 529 nm

Parameter	1	2	3	4	5	6	7
FBG $\Delta\lambda$ /pm	62.3	61.6	61.1	62.0	61.6	62.2	61.8
Strain gauge $\Delta\epsilon$ / $\mu\epsilon$	50.6	50.6	50.3	50.3	50.4	50.4	50.4
Sensitivity coefficient/ (pm· $\mu\epsilon^{-1}$)	1.23	1.22	1.22	1.23	1.22	1.23	1.23

表3 1 547 nm波长的FBG应变传感器和电阻应变片波峰值
Table 3 Peak value of FBG strain sensor and resistance strain gauge at 1 547 nm

Parameter	1	2	3	4	5	6	7
FBG $\Delta\lambda/\text{pm}$	59.7	60.8	59.6	59.9	59.9	59.6	60.8
Strain gauge $\Delta\epsilon/\mu\epsilon$	50.6	50.6	50.3	50.3	50.4	50.4	50.4
Sensitivity coefficient/ ($\text{pm}\cdot\mu\epsilon^{-1}$)	1.18	1.20	1.18	1.19	1.19	1.18	1.21

重复悬挂砝码的过程一共测试3次,得到其灵敏度校准系数如表4所示,250 g砝码激励下1 529 nm和1 547 nm波长的FBG应变传感器动态校准实验3次测量的平均值分别为1.230 $\text{pm}/\mu\epsilon$ 和1.193 $\text{pm}/\mu\epsilon$,其相对标准差最大仅为0.88%,说明实验结果的一致性和重复性良好。

表4 250 g砝码激励下的FBG应变传感器灵敏度校准系数
Table 4 Sensitivity calibration coefficient of FBG strain sensor under 250 g weight excitation

Wavelength/ nm	First test		Second test		Third test		Average value
	Sensitivity coefficient/ ($\text{pm}\cdot\mu\epsilon^{-1}$)	Relative standard deviation	Sensitivity coefficient/ ($\text{pm}\cdot\mu\epsilon^{-1}$)	Relative standard deviation	Sensitivity coefficient/ ($\text{pm}\cdot\mu\epsilon^{-1}$)	Relative standard deviation	Sensitivity coefficient/ ($\text{pm}\cdot\mu\epsilon^{-1}$)
1 529	1.23	0.57%	1.23	0.58%	1.23	0.66%	1.230
1 547	1.19	0.88%	1.19	0.46%	1.20	0.26%	1.193

当在悬臂梁末端瞬间悬挂一个重量为500 g的砝码时,按照相同的处理方法计算FBG应变传感器的灵敏度校准系数。重复悬挂砝码的过程一共测试3次,得到其灵敏度校准系数如表5所示,500 g砝码激励下1 529 nm和1 547 nm波长的FBG应变传感器动态校准实验3次测量的平均值分别为1.230 $\text{pm}/\mu\epsilon$ 和1.193 $\text{pm}/\mu\epsilon$,其相对标准差最大仅为0.66%,实验结果的一致性和重复性良好。

表5 500 g砝码激励下的FBG应变传感器灵敏度校准系数
Table 5 Sensitivity calibration coefficient of FBG strain sensor under 500 g weight excitation

Wavelength/ nm	First test		Second test		Third test		Average value
	Sensitivity coefficient/ ($\text{pm}\cdot\mu\epsilon^{-1}$)	Relative standard deviation	Sensitivity coefficient/ ($\text{pm}\cdot\mu\epsilon^{-1}$)	Relative standard deviation	Sensitivity coefficient/ ($\text{pm}\cdot\mu\epsilon^{-1}$)	Relative standard deviation	Sensitivity coefficient/ ($\text{pm}\cdot\mu\epsilon^{-1}$)
1 529	1.23	0.40%	1.23	0.66%	1.23	0.49%	1.230
1 547	1.20	0.31%	1.19	0.32%	1.19	0.26%	1.193

由结果对比分析可得,在不同重量砝码的动态激励作用下,1529 nm和1547 nm波长的FBG应变传感器动态校准结果基本一致,因此不同的动态激励下,该方法都能较好地校准FBG应变传感器,具有较高的准确性。

将1 529 nm和1 547 nm的两个FBG应变传感器在实验室条件下进行静态砝码标定,实验装置与图2基本相同,不同的是静态标定是在等强度悬臂梁末端依次施加5个砝码以提供静态应变值,将FBG应变传感器的波长值与电阻应变片的应变值进行直线拟合,直线的拟合度达到了0.99,静态标定结果如图5所示,重复实验5次取平均值,得到1 529 nm和1 547 nm波长的FBG应变传感器静态灵敏度校准系数分别为1.23 $\text{pm}/\mu\epsilon$ 和1.20 $\text{pm}/\mu\epsilon$,其相对标准差仅为0.4%。有初始值的情况下,1 529 nm和1 547 nm波长的FBG应变传感器动态灵敏度校准系数分别为1.230 $\text{pm}/\mu\epsilon$ 和1.193 $\text{pm}/\mu\epsilon$,动态校准结果与静态标定结果基本相同,因此该方法可用于FBG应变传感器的原位动态校准。

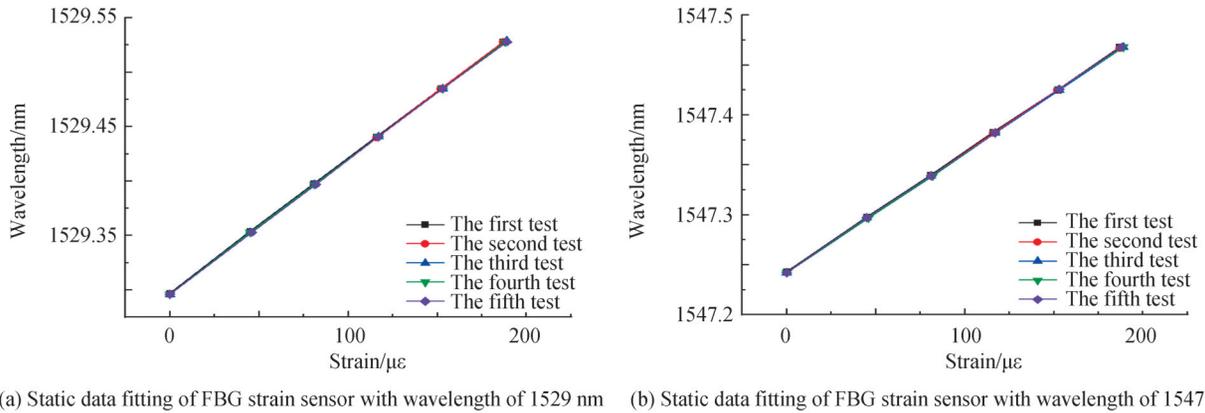


图5 波长为 1 529 nm 和 1 547 nm 的 FBG 应变传感器的静态数据拟合
Fig.5 Static data fitting of FBG strain sensors with wavelength of 1 529 nm and 1 547 nm

4 结论

针对动态工况下 FBG 应变传感器测量桥梁结构应变值的准确性问题,本文提出了一种动态激励下的 FBG 应变传感器原位校准方法。采用不同重量的砝码作为动态激励源,利用互相关算法对两组数据波形进行匹配,解决时间错位问题,然后在 FBG 应变传感器和电阻应变片有初始值的情况下,将两者波峰值的比值作为 FBG 应变传感器的灵敏度校准系数。实验结果表明:不同重量的砝码作为激励源对于校准结果没有影响,1 529 nm 和 1 547 nm 波长的 FBG 应变传感器的灵敏度校准系数分别为 $1.230 \text{ pm}/\mu\epsilon$ 和 $1.193 \text{ pm}/\mu\epsilon$,与静态标定结果基本相同,因此该方法可用于 FBG 应变传感器的原位动态校准。

参考文献

- [1] WU B, LU H, BO C. Study on finite element model updating in highway bridge static loading test using spatially-distributed optical fiber sensors[J]. Sensors, 2017, 17(7): 1657-1674.
- [2] WANG L, XIN X, SONG J, et al. Finite element analysis-based study of fiber Bragg grating sensor for cracks detection in reinforced concrete[J]. Optical Engineering, 2018, 57(2): 027103.
- [3] HUANG F, CHEN T, SI J, et al. Fiber laser based on a fiber Bragg grating and its application in high-temperature sensing [J]. Optics Communications, 2019, 452: 233-237.
- [4] BAI Shengbao, XIAO Yingchun, HUANG Bo, et al. Research on strain calibration method of fiber Bragg grating sensor [J]. Journal of Vibration, Measurement & Diagnosis, 2016, 36(2): 321-324.
白生宝, 肖迎春, 黄博, 等. FBG 传感器应变标定方法[J]. 振动. 测试与诊断, 2016, 36(2): 321-324.
- [5] SHANG Q, QIN W. Fiber Bragg grating dynamic calibration based on online sequential extreme learning machine [J]. Sensors (Basel, Switzerland), 2020, 20(7): 1840-1851.
- [6] LIU W, WANG B, ZHOU Z, et al. Design and testing of a large-scale shape-monitoring sensor based on fiber-Bragg-grating sensing technique for pavement structure[J]. Journal of Transportation Engineering, Part A: Systems, 2017, 143(5): 04017009.
- [7] JIANG Shu, LI Tao, LIN Jiejun, et al. Development and application of the FBG strain sensor for ship[J]. Chinese Journal of Scientific Instrument, 2020, 41(6): 35-42.
江舒, 李涛, 林杰俊, 等. 船用光纤光栅应变传感器开发与应用研究[J]. 仪器仪表学报, 2020, 41(6): 35-42.
- [8] FUJII Y. Toward establishing dynamic calibration method for force transducers[J]. IEEE Transactions on Instrumentation and Measurement, 2009, 58(7): 2358-2364.
- [9] TAN R, CHEN C, ZHENG Y, et al. High-precision calibration method for fiber Bragg grating strain sensing based on an optical lever[J]. Optical Fiber Technology, 2020, 61(3): 102392.
- [10] JIN Ran, LV Xiang, CHEN Wei, et al. Shock calibration device including laser velocimeter for dynamic characteristics of strain sensor[J]. Journal of Astronautic Metrology and Measurement, 2021, 41(3): 38-42.
金冉, 吕翔, 陈伟, 等. 应变传感器动态特性激光绝对法冲击校准装置[J]. 宇航计测技术, 2021, 41(3): 38-42.
- [11] YU S J, YANG J X, CHEN J Y. The fiber Bragg grating sensor and its interrogator for dynamic strain measurement of concrete[J]. Advanced Materials Research, 2013, 655-657: 679-683.
- [12] JIANG Chengcheng. Development of FBG strain sensor calibration system based on equal strength beam [D]. Xiamen: Xiamen University, 2019.
江承成. 基于等强度梁的 FBG 应变传感器标定系统开发[D]. 厦门: 厦门大学, 2019.

- [13] HuiminQI, CAO Shengmin. Application of strain measurement in marine pile static load test [J]. Port Engineering Technology, 2011, 48(3): 54-58.
裘惠民, 曹胜敏. 应变测量在海上桩基静载试验中的应用[J]. 港工技术, 2011, 48(3): 54-58.
- [14] XUE Yuanze, WANG Xuefeng, TANG Caijie, et al. Cross-correlation algorithm of optical frequency domain reflectometry sensing system based on adapted range[J]. Acta Optica Sinica, 2021, 41(13): 1306020.
薛渊泽, 王学锋, 唐才杰, 等. 自适应量程的光频域反射光纤传感互相关算法[J]. 光学学报, 2021, 41(13): 1306020.
- [15] KONECNY J, KROMER P, PRAUZEK M, et al. Scan matching by cross-correlation and differential evolution [J]. Electronics, 2019, 8(8): 856.

In-situ Calibration Method of FBG Strain Sensor under Dynamic Excitation

LU Ye¹, GONG Huaping¹, CAI Jingyi¹, FAN Qiming², ZHAO Chunliu¹

(1 Institute of Optoelectronic Technology, China Jiliang University, Hangzhou 310018, China)

(2 Institute of Optics and Laser Metrology, National Institute of Metrology, Beijing 100029, China)

Abstract: Strain monitoring is important for structural health monitoring of bridges, dams, high-rise buildings and so on. The metrological performance of strain sensing systems is an important guarantee for the accuracy of structural monitoring data. Common sensors for strain monitoring include Fiber Bragg grating strain sensors, resistive strain gauges, and vibrating wire strain gauges. Fibre Bragg grating strain sensors have the advantages of strong anti-electromagnetic interference, high precision, good durability, and distributed measurement. They have a large number of applications in the field of engineering construction and instrumentation. Fibre Bragg grating strain sensors usually work under dynamic conditions during bridge health monitoring. If the sensor measurement data is incorrect, it will have a negative impact on subsequent control, monitoring and fault diagnosis systems. Therefore, it is necessary to perform on-site calibration of the Fiber Bragg grating strain sensor in actual use to ensure the accuracy of the measurement results. At present, there are mainly two methods for on-site calibration of Fiber Bragg grating strain sensors: static calibration and dynamic calibration. In the actual bridge inspection, static calibration must block traffic operation for a period of time, which will have a certain impact on social and economic life, while dynamic calibration has little effect on traffic operation, so it is necessary to perform dynamic calibration of Fiber Bragg grating strain sensors. Aiming at the accuracy of fiber grating strain sensor in measuring dynamic strain value of bridge structure, a calibration method of Fibre Bragg grating strain sensor under dynamic excitation is proposed. The equal-strength cantilever beam is used to simulate the bridge structure, and weights of different weights are suspended instantaneously at the end of the equal-strength cantilever beam to simulate the dynamic excitation generated by the vehicle on the bridge. The resistance strain gauge has a simple structure, high output accuracy and good stability and is suitable for use as a standard sensor for the transmission of strain values. Therefore, a high-precision resistance strain gauge is selected as the reference sensor. The resistance strain gauge is used as the reference sensor, and the Fiber Bragg grating strain sensor is used as the sensor to be calibrated, and the measurement data sequences of the reference sensor and the sensor to be calibrated are compared. The premise of dynamic calibration is that the changes of the magnitude waveform of the sensor to be calibrated and the reference sensor under the same excitation source are basically the same. If the waveform of the two magnitude sequences is poorly matched, the dynamic calibration of the sensor cannot be performed. Because the sampling start time of the reference sensor and the sensor to be calibrated are not synchronized, and their own characteristics are different, the change waveform of the two measured value sequences will appear time misalignment. Therefore, in view of the time dislocation problem in the measurement data sequence, a cross-correlation algorithm is used to match the measurement data of the reference sensor and the sensor to be calibrated. Then, when the Fiber Bragg grating strain sensor has the initial value, the measurement value calibration is studied. When the Fiber Bragg grating strain sensor and the resistance strain gauge have the initial value, the ratio of the wave peak value of the two is used as the sensitivity calibration coefficient of the Fiber Bragg grating strain sensor. The experimental results show that the method effectively solves

the time dislocation problem of the measurement data sequence, the data matching rate is more than 98%, and the dynamic calibration of the fiber grating strain sensor is realized. The use of different weights as the excitation source does not effect the calibration results. The sensitivity calibration coefficients of Fiber Bragg grating strain sensors at 1 529 nm and 1 547 nm wavelengths are basically consistent with the static calibration results.

Key words: Fiber Bragg grating; Dynamic calibration; Data sequence matching; Strain sensor; Data dislocation

OCIS Codes: 060.2300; 060.2340; 060.2370; 060.3735